21st International Symposium on
Mathematical Theory of Networks and Systems
July 7-11, 2014. Groningen, The Netherlands

An observer-based approach for thermoacoustic tomography

Ghislain HAINE
Université de Toulouse; ISAE, DMIA; F-31055 Toulouse, France
Funded by "IDEX-nouveaux entrants"
Email: Ghislain.haine@isae.fr

Abstract

We propose to use the observer-based algorithm of Ramdani, Tucsnak and Weiss [29] for the initial state recovery of the wave equation involved in thermoacoustic tomography. We proved the rate of convergence of the iterative algorithm to the observable part *of the initial state. We performed 3D numerical test in the relevant case where the measurement is performed on a grid of transducers on a half-sphere.*

1. Introduction

In medical imaging, we mostly need to recover the initial (or final) state of a physical system from partial observation over some finite time interval. In general, measurements are performed outside the body. This constraint leads to incomplete data. For instance in breast or kidney imaging, we cannot expect a measurement all around the object of interest. In this paper we investigate the problem of data recovery with this lack of information. In other words, we investigate systems which are not *exactly observable* (more than one initial state lead to the same observation).

In the last decade, new algorithms based on time reversal (see Fink [9, 10]) have been proposed for data recovery. We can mention, for instance, the Back and Forth Nudging proposed by Auroux and Blum [2], the Time Reversal Focusing by Phung and Zhang [27], the algorithm proposed by Ito, Ramdani and Tucsnak [18] and finally, the one we will consider in this paper, the algorithm studied in [29].

In thermoacoustic tomography, the problem is to recover the initial state of a wave equation from surface measurements (see Gebauer and Scherzer [12]). For mathematical issues related to this medical imaging technique, see for instance the survey of Kuchment and Kunyansky [19].

Various methods have been used to tackle the problem of thermoacoustic tomography, such as inverse source concepts in Fourier domain [1], Fourier series [20, 21, 22] and time reversal method [17]. A new method has been proposed in [30], based on time reversal and leading to a Neumann series. It has been studied in recent works [28, 26]. Finally, observer-based algorithm for data assimilation [2] has been successfully applied to thermoacoustic tomography [3].

We propose the use of the iterative observer-based algorithm of [29], which also leads to a Neumann series as it is proven in Proposition 2.2. However, it involves only the resolution of direct wave equations in practice. Our main result, Theorem 2.1, shows that the algorithm converges at least polynomially to the initial state. Moreover, in the case of incomplete data, we prove that it converges to the *observable part* of the initial state.

Let us state our mathematical inverse problem. We consider the wave equation in the whole domain $\mathbb{R}^3$, with initial position compactly supported in a bounded open set $\Omega \subset \mathbb{R}^3$. More precisely, let $w_0 \in H_0^1(\Omega)$, and consider the following system

$$\begin{cases} \dfrac{\partial^2}{\partial t^2} w(x,t) = \Delta w(x,t), & \forall x \in \mathbb{R}^3, t \geq 0, \\ w(x,0) = w_0(x), & \forall x \in \Omega, \\ w(x,0) = 0, & \forall x \in \mathbb{R}^3 \setminus \Omega, \\ \dfrac{\partial}{\partial t} w(x,0) = 0, & \forall x \in \mathbb{R}^3. \end{cases} \tag{1}$$

The observation is performed on a surface surrounded the initial state. We then suppose that we observe the state w on $\partial\Omega$, during a time interval $[0,\tau]$, with $\tau \geq \operatorname{diam}(\Omega)$, where $\operatorname{diam}(\Omega)$ is the supremum of the path rays from boundary to boundary Ω (see typical configuration on Fig. 1). This last assumption will lead to a well-posed inverse problem. However, our method allows to consider ill-posed cases. For instance, we could observe only on a part of the boundary, as it is done in the numerical tests.

ISBN: 978-90-367-6321-9

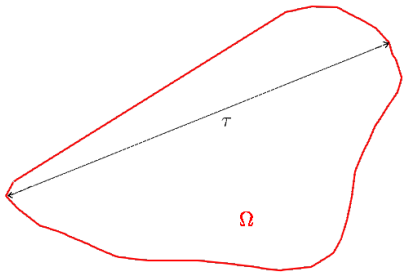

Figure 1: Cut in the plane containing diam(Ω) of an example of configuration.

The paper is organized as follows. In Section 2, we described the algorithm of [29] and state Theorem 2.1. In Section 3, we prove that thermoacoustic tomography fits into our framework, and leads to a well-posed inverse problem when we observe on a closed surface surrounding the body. In Section 4, we test the accuracy of this method, with both complete and partial observation, in presence of white noise.

2. The observer-based algorithm

Let X be Hilbert spaces and A be a skew-adjoint operator on X. We investigate the initial state recovery of

$$\begin{cases} \dot{z}(t) = Az(t), \quad \forall t \geq 0, \\ z(0) = z_0 \in X. \end{cases} \tag{2}$$

Such systems are often used to model vibrating systems (acoustic or elastic waves) or quantum systems (Schrödinger equations).

Let Y be another Hilbert space and $C \in \mathscr{L}(X,Y)$. We suppose that we have access to z through the operator C, during a time interval $[0,\tau]$, $\tau > 0$, leading to

$$y(t) = Cz(t), \quad \forall t \in [0,\tau]. \tag{3}$$

We call C the observation operator.

For systems described by evolution partial differential equations (*i.e.* when A is a differential operator in the space variables on a domain Ω), $C \in \mathscr{L}(X,Y)$ generally correspond to measurement on a subdomain $\mathscr{O} \subset \Omega$, as unbounded observation operator correspond mostly to measurement on the boundary of Ω. We will see that the observation operator corresponding to thermoacoustic tomography is bounded, *i.e.* $C \in \mathscr{L}(X,Y)$.

Let Ψ_τ be the operator which maps z_0 on y. The inverse problem is well-posed when Ψ_τ is left-invertible, with continuous inverse. This will be the case if and only if Ψ_τ is bounded from below

$$\exists k_\tau > 0, \quad \|\Psi_\tau z_0\| \geq k_\tau \|z_0\|, \quad \forall z_0 \in X. \tag{4}$$

The pair (A,C) is said to be *exactly observable in time* τ when relation (4) holds.

Let us introduce the algorithm proposed by Ramdani, Tucsnak and Weiss [29] in the particular case of a skew-adjoint generator and bounded observation operator, when (A,C) is exactly observable in time $\tau > 0$. Let $\mathbb{T}^+$ (respectively $\mathbb{T}^-$) be the exponentially stable C_0-semigroup generated by $A^+ = A - \gamma C^*C$ (respectively $A^- = -A - \gamma C^*C$), for some $\gamma > 0$ (see Liu [23]). For all $n \in \mathbb{N}^*$, we define the following systems (called respectively the *forward and backward observers*)

$$\begin{cases} \dot{z}_n^+(t) = A^+ z_n^+(t) + \gamma C^* y(t), \quad \forall t \in [0,\tau], \\ z_1^+(0) = z_0^+ \in X, \\ z_n^+(0) = z_{n-1}^-(0), \quad \forall n \geq 2, \end{cases} \tag{5}$$

$$\begin{cases} \dot{z}_n^-(t) = -A^- z_n^-(t) - \gamma C^* y(t), \quad \forall t \in [0,\tau], \\ z_n^-(\tau) = z_n^+(\tau), \quad \forall n \geq 1. \end{cases} \tag{6}$$

The forward error $e_n^+(t) = z_n^+(t) - z(t)$ verifies

$$\begin{cases} \dot{e}_n^+(t) = (A - \gamma C^*C) e_n^+(t), \quad \forall t \in [0,\tau], \\ e_1^+(0) = z_0^+ - z_0 \in X, \\ e_n^+(0) = e_{n-1}^-(0), \quad \forall n \geq 2, \end{cases}$$

and the backward error $e_n^-(t) = z_n^-(t) - z(t)$ verifies

$$\begin{cases} \dot{e}_n^-(t) = (A + \gamma C^*C) e_n^-(t), \quad \forall t \in [0,\tau], \\ e_n^-(\tau) = e_n^+(\tau), \quad \forall n \geq 1. \end{cases}$$

So, we have

$$\left\| z_n^-(0) - z_0 \right\| \leq \left\| \mathbb{T}_\tau^- \mathbb{T}_\tau^+ \right\|^n \left\| z_0^+ - z_0 \right\|. \tag{7}$$

According to Ito, Ramdani and Tucsnak [18, Lemma 2.2] we have $\alpha = \|\mathbb{T}_\tau^- \mathbb{T}_\tau^+\|_{\mathscr{L}(X)} < 1$ and thus

$$\|z_n^-(0) - z_0\| \leq \alpha^n \|z_0^+ - z_0\| \underset{n\to\infty}{\longrightarrow} 0.$$

In the case of exactly observable systems, we call systems (5)–(6) *forward and backward observers* as it is a generalization to infinite dimensional systems of the so-called Luenberger's observer [24], well-known in control theory.

If we drop the exact observability assumption, we get the following result.

Theorem 2.1 *Let X and Y be Hilbert spaces. Assume that A is a skew-adjoint operator on X and $C \in \mathscr{L}(X,Y)$. Denote by $A^+ = A - \gamma C^*C$ and $A^- = -A - \gamma C^*C$ for some $\gamma > 0$ and z_n^+ and z_n^- the solutions of (5) and (6) respectively, and let $\Psi_\tau \in \mathscr{L}(X, L^2([0,\tau),Y))$ be the operator which maps z_0 on y (via (3)). Furthermore, we denote by Π the orthogonal projector from X onto $(\operatorname{Ker}\Psi_\tau)^\perp$, then we have for all $z_0 \in X$, $z_0^+ \in (\operatorname{Ker}\Psi_\tau)^\perp$:*

1. $z_n^-(0) \in (\mathrm{Ker}\,\Psi_\tau)^\perp$ *for all* $n \geq 1$ *and*

$$\left\|(I-\Pi)\left(z_n^-(0)-z_0\right)\right\| = \|(I-\Pi)z_0\|.$$

2. *The sequence* $\left(\|z_n^-(0)-\Pi z_0\|\right)_{n\geq 1}$ *verifies*

$$\left\|z_n^-(0)-\Pi z_0\right\| = o\left(\frac{1}{n}\right).$$

3. *The convergence is exponential, i.e. there exists a constant* $\alpha \in (0,1)$*, independent of* z_0 *and* z_0^+*, such that*

$$\left\|z_n^-(0)-\Pi z_0\right\| \leq \alpha^n \left\|z_0^+-\Pi z_0\right\|, \quad \forall n \geq 1,$$

if and only if Ψ_τ *is bounded from below on* $(\mathrm{Ker}\,\Psi_\tau)^\perp$.

Remark 2.1 *In practice, it is not easy to characterize the kernel* $\mathrm{Ker}\,\Psi_\tau$*. However, it is often possible to characterize a subspace of this kernel, and from this a class of initial data* z_0 *the algorithm can reconstruct. Furthermore, the first guess* z_0^+ *can be taken equal to zero, ensuring the assumption* $z_0^+ \in (\mathrm{Ker}\,\Psi_\tau)^\perp$*. Then, starting from zero and identifying a class of available initial data, we do not need to know* Π *anymore.*

The only part of the theorem that is not proved in [14] is the polynomial rate of convergence.

Let $L = \mathbb{T}_\tau^- \mathbb{T}_\tau^+|_{(\mathrm{Ker}\,\Psi_\tau)^\perp}$. From [14], we know that $L \in \mathscr{L}\left((\mathrm{Ker}\,\Psi_\tau)^\perp\right)$ is a positive self-adjoint operator, satisfying $\|Lz\| < \|z\|$ for all $z \in (\mathrm{Ker}\,\Psi_\tau)^\perp \setminus \{0\}$. Furthermore, we have

$$\left\|z_n^-(0)-\Pi z_0\right\| = \|L^n\left(z_0^+-\Pi z_0\right)\|.$$

Let $z \in (\mathrm{Ker}\,\Psi_\tau)^\perp$, $\|z\| = 1$. Since $\|L^{n+1}z\| < \|L^n z\|$ we have

$$\begin{aligned} &\|L^{n+1}z\| < \|L^n z\| \\ &\Rightarrow \frac{1}{n+1}\ln\|L^{n+1}z\| < \frac{1}{n}\ln\|L^n z\| \\ &\Leftrightarrow \|L^{n+1}z\|^{\frac{1}{n+1}} < \|L^n z\|^{\frac{1}{n}}. \end{aligned}$$

So that the sequence defined by $u_0 = 1$ and $u_n = \left\|L^n \frac{z}{\|z\|}\right\|^{\frac{1}{n}}$ for $n \geq 1$ is strictly decreasing and thus converges in $[0,1)$, for all $z \in (\mathrm{Ker}\,\Psi_\tau)^\perp$. From Cauchy's rule, $\sum_{n=0}^\infty L^n z = \|z\| \sum_{n=0}^\infty L^n \frac{z}{\|z\|}$ is absolutely convergent. In particular $\|L^n z\| = o\left(\frac{1}{n}\right)$, for all $z \in (\mathrm{Ker}\,\Psi_\tau)^\perp$.

Proposition 2.2 *Under the assumptions and notation of Theorem 2.1, suppose that* $z_0^+ = 0$*. Denote by* $z^-(0)$ *the first approximation of* z_0 *obtain after one forward-backward cycle of (5)–(6). Then we have*

$$\Pi z_0 = \sum_{n=0}^\infty L^n z_1^-(0). \tag{8}$$

Remark 2.2 *Thus, at least theoretically, the reconstruction of the observable part of the initial state is given by (8). Note that the computation of the first term in the above sum requires to solve the two non-homogeneous systems (5) and (6), while the terms for* $n \geq 1$ *involve the resolution of the two homogeneous systems associated with (5) and (6) (i.e. for* $y \equiv 0$*). In practice, this leads to a gain in computation time.*

Let $z_0^+ = 0$. After one forward–backward cycle of (5)–(6), we have

$$\mathbb{T}_\tau^- \mathbb{T}_\tau^+ z_0 = z_0 - z^-(0).$$

Taking the projection on $(\mathrm{Ker}\,\Psi_\tau)^\perp$ and using [14, Corollary 3.7], we get

$$(I-L)\Pi z_0 = z^-(0).$$

So that if we can invert the operator $(I-L)$, we obtain

$$\Pi z_0 = (I-L)^{-1} z^-(0).$$

If $\|L\| < 1$, the result is trivial, but it can be equal to 1. However, in the proof of Theorem 2.1, we saw that

$$\sum_{n=0}^\infty L^n z, \quad \forall z \in (\mathrm{Ker}\,\Psi_\tau)^\perp,$$

is absolutely convergent. An easy computation shows that this is the inverse of $(I-L)$.

3. Application to Thermoacoustic Tomography

The main difficulty is that the problem is set on the whole space, and thus we cannot expect to obtain exact observability (because of geometric optic conditions of Bardos, Lebeau and Rauch [4]).

Let us start by the addition of boundary conditions on a *sufficiently large* bounded domain. Thus we will be able to rewrite the problem in the suitable abstract form (2)–(3).

When $w_0 \in C^\infty(\mathbb{R}^3)$, the solution of (1) is given by the well-known Poisson-Kirchhoff formula [8, p. 72 equation (21)]

$$w(x,t) = \frac{\partial}{\partial t}\left(tSw_0(x)\right), \quad \forall x \in \mathbb{R}^3, t \geq 0, \tag{9}$$

where $Sf(x,t) = \int_{|v|=1} f(x+tv)d\sigma(v)$ is the spherical mean operator. In particular, this formula implies that the solution is supported in $\Omega_t = \{y \in \mathbb{R}^3 \mid |x-y| \leq t, x \in \Omega\}$, for all $t \geq 0$. This phenomena is known as Huygens' principle [8, p. 80]. We can thus add an artificial condition (for instance Dirichlet condition) on the boundary of

$$\Omega_{\tau^+} = \{y \in \mathbb{R}^3 \mid |x-y| \leq \tau + \varepsilon, x \in \Omega\},$$

for some fixed $\varepsilon > 0$, and get that the solution of (1) is also the solution of (until time $\tau + \varepsilon$)

$$\begin{cases} \dfrac{\partial^2}{\partial t^2} w(x,t) = \Delta w(x,t), & \forall x \in \Omega_{\tau^+}, t \in [0,\tau], \\ w(x,t) = 0, & \forall x \in \partial\Omega_{\tau^+}, t \in [0,\tau], \\ w(x,0) = w_0(x), & \forall x \in \Omega, \\ w(x,0) = 0, & \forall x \in \Omega_{\tau^+} \setminus \Omega, \\ \dfrac{\partial}{\partial t} w(x,0) = 0, & \forall x \in \Omega_{\tau^+}. \end{cases} \tag{10}$$

Of course, for $t \leq \tau$, the Poisson-Kirchhoff formula remains true. In the sequel, we denote by w both the solutions of (1) and (10).

Let $\gamma_0 \in \mathscr{L}\left(H_0^1(\Omega_{\tau^+}), H^{\frac{1}{2}}(\partial\Omega)\right)$ be the Dirichlet trace operator. We define

$$\mathscr{D}(A_0) = H^2(\Omega_{\tau^+}) \cap H_0^1(\Omega_{\tau^+}), \qquad H = L^2(\Omega_{\tau^+}),$$

$$A_0 = -\Delta : \mathscr{D}(A_0) \longrightarrow H,$$

and

$$\mathscr{D}\left(A_0^{\frac{1}{2}}\right) = H_0^1(\Omega_{\tau^+}) \to H^{\frac{1}{2}}(\partial\Omega), \qquad Y = L^2(\partial\Omega),$$

$$C_0 = \gamma_0 : \mathscr{D}\left(A_0^{\frac{1}{2}}\right) \to H^{\frac{1}{2}}(\partial\Omega) \hookrightarrow Y.$$

We can rewrite (10) (we forget the assumption on the support of w_0 here)

$$\begin{cases} \ddot{w}(t) + A_0 w(t) = 0, & \forall t \in [0,\tau], \\ w(0) = w_0 \in \mathscr{D}\left(A_0^{\frac{1}{2}}\right), \\ \dot{w}(0) = w_1 \in H. \end{cases}$$

As our algorithm (5)–(6) is written for first-order systems, we also introduce the following definitions

$$z(t) = \begin{bmatrix} w(t) \\ \dot{w}(t) \end{bmatrix}, \qquad X = \mathscr{D}\left(A_0^{\frac{1}{2}}\right) \times H,$$

$$A = \begin{pmatrix} 0 & I \\ -A_0 & 0 \end{pmatrix}, \qquad \mathscr{D}(A) = \mathscr{D}(A_0) \times \mathscr{D}\left(A_0^{\frac{1}{2}}\right),$$

$$C \in \mathscr{L}(X,Y), \qquad C = \begin{bmatrix} C_0 & 0 \end{bmatrix},$$

to obtain

$$\begin{cases} \dot{z}(t) = Az(t), & \forall t \in [0,\tau], \\ z(0) = z_0 \in X, \end{cases}$$

and

$$y(t) = Cz(t), \quad \forall t \in [0,\tau].$$

It is clear that A is skew-adjoint, C is bounded, but (A,C) is not exactly observable in time τ in general. Indeed, there exists configurations where the geometric optic condition of Bardos, Lebeau and Rauch [4] fails, as on Fig. 2. We define the observers z_n^+ and z_n^- by (5)-

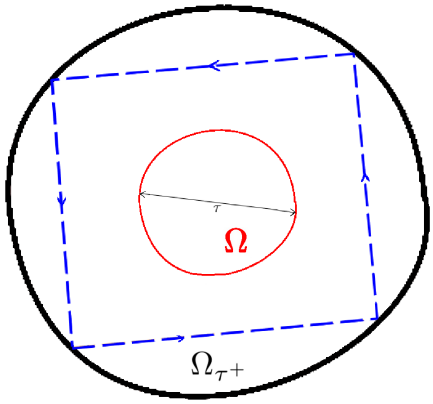

Figure 2: Cut in the plane containing $\mathrm{diam}(\Omega)$ of an example of configuration, with artificial boundary condition, without exact observability: the dashed ray is trapped.

(6), for some gain parameter $\gamma > 0$, using the operators

$$A^+ = \begin{pmatrix} -\gamma C_0^* C_0 & I \\ -A_0 & 0 \end{pmatrix}, \quad A^- = \begin{pmatrix} -\gamma C_0^* C_0 & -I \\ A_0 & 0 \end{pmatrix}.$$

On second order form, *i.e.* with

$$z_n^+(t) = \begin{bmatrix} w_n^+(t) \\ \widetilde{w}_n^+(t) \end{bmatrix}, \quad z_n^-(t) = \begin{bmatrix} w_n^-(t) \\ \widetilde{w}_n^-(t) \end{bmatrix},$$

the observers (5)–(6) take the following form

$$\begin{cases} \dot{w}_n^+(t) = -\gamma C_0^* C_0 w_n^+(t) \\ \qquad + \widetilde{w}_n^+(t) + \gamma C_0^* y(t), & \forall t \in [0,\tau], \\ \dot{\widetilde{w}}_n^+(t) = -A_0 w_n^+(t), & \forall t \in [0,\tau], \\ w_1^+(0) = 0, \\ \widetilde{w}_1^+(0) = 0, \\ w_n^+(0) = w_{n-1}^-(0), & \forall n \geq 2, \\ \widetilde{w}_n^+(0) = \widetilde{w}_{n-1}^-(0), & \forall n \geq 2, \end{cases} \tag{11}$$

$$\begin{cases} \dot{w}_n^-(t) = \gamma C_0^* C_0 w_n^-(t) \\ \qquad + \widetilde{w}_n^-(t) - \gamma C_0^* y(t), & \forall t \in [0,\tau], \\ \dot{\widetilde{w}}_n^-(t) = -A_0 w_n^-(t)(t), & \forall t \in [0,\tau], \\ w_n^-(\tau) = w_n^+(\tau), & \forall n \geq 1, \\ \widetilde{w}_n^-(\tau) = \widetilde{w}_n^+(\tau), & \forall n \geq 1. \end{cases} \tag{12}$$

Note that $\dot{w}_n^{\pm}(t) = \widetilde{w}_n^{\pm}(t)$ correspond to the case when $\gamma \to \infty$ (see Chapelle, Cîndea, De Buhan and Moireau [5] for more details on this type of observers). However, it is well-known (see for instance [16, 25]) that there exists an optimal value for γ, with an overdamping phenomena for larger choice. Of course, this optimal value depends on the observation surface, and we expect it to be different for the three cases we will test in the following section.

It remains to show that the compactly supported initial state considered in thermoacoustic tomography belongs to $(\operatorname{Ker}\Psi_\tau)^\perp$ to apply Theorem 2.1.

Suppose that $w_0 \in C_0^\infty(\Omega_{\tau^+})$ is compactly supported in Ω (which can be supposed connected without loss of generality) and leads to an output $y \equiv 0$, *i.e.* that $(w_0, 0) \in (C_0^\infty(\Omega_{\tau^+}) \times \{0\}) \cap \operatorname{Ker}\Psi_\tau$. Then the solution of (1) verifies

$$w(x,t) = 0, \quad \forall x \in \partial\Omega, t \in [0,\tau].$$

From Poisson-Kirchhoff formula (9), we easily show that

$$\begin{aligned} w(x,t) = 0, \quad \forall x \in \partial\Omega, t \in [0,\tau] \\ \implies \quad Sw_0(x)(t) = 0, \quad \forall x \in \partial\Omega, t \geq 0, \end{aligned}$$

where S is the spherical mean operator. Then we apply [19, Corollary 2] to prove injectivity

$$Sw_0(x)(t) = 0, \quad \forall x \in \partial\Omega, t \geq 0 \quad \implies \quad w_0 \equiv 0.$$

We conclude by the density of $C_0^\infty(\Omega_{\tau^+})$ in $H_0^1(\Omega_{\tau^+})$.

4. Numerical simulations

We implement the algorithm on GMSH [13] and GetDP [6] to test the accuracy of our approach. To speed up the time resolution, we use the formula (8) (GetDP is optimized for the resolution of homogeneous linear problems). The optimal value for the gain parameter is a difficult issue (see [16] for the string equation case), we then perform different simulations in each case and select the best for the corresponding observation (we tested $\gamma = 1$, 5, 15 and 30).

In these first tests performed on a coarse mesh, we observe on a sphere of radius 0.5 surrounding the support of the initial data to recover, with gain parameter $\gamma = 5$. We add Gaussian noise to the observation, with 0.25 of deviation.

We see that this algorithm is quite efficient on Fig. 3, even with the white noise that is not taken into account in the theoretical framework. After 10 iterations, we reached less than 5% of relative error in L^2.

In practice, it is not relevant to measure on a surface surrounding the initial state. We know from Theorem 2.1 that the observer-based algorithm will converge to the observable part of the initial data in any case. Suppose now that we observe only on a half-sphere, since the initial velocity is null, the information spread out in all directions, and we can hope, intuitively, to reconstruct some non null part of the initial data. This is what we tested in the next simulation. We use the same mesh and the same observation, but truncated on a half-sphere, and the same gain parameter $\gamma = 5$. We see on Fig. 4 that the initial state, despite the lack of observation, is quite well reconstructed. We reached near to 20% of relative error in L^2. Of course, we cannot expect a full reconstruction. A further investigation has to be done to know exactly what is loss in this case. In other words, $(\operatorname{Ker}\Psi_\tau)^\perp$ has to be explicitly constructed.

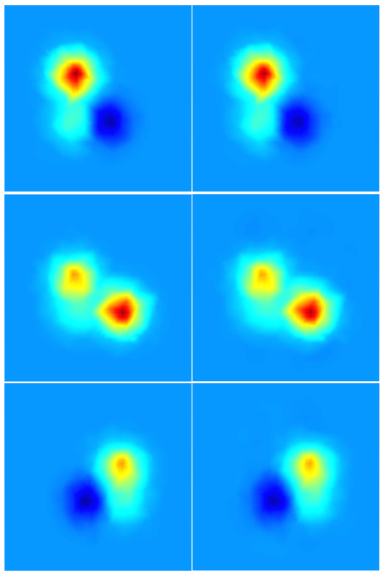

Figure 3: Initial state (left) and the reconstructed state (right) from complete data after 10 iterations. This pictures are obtained from the three planes XY, YZ and XZ, passing by $(-0.125, -0.125, -0.125)$. The color scale are the same for all pictures.

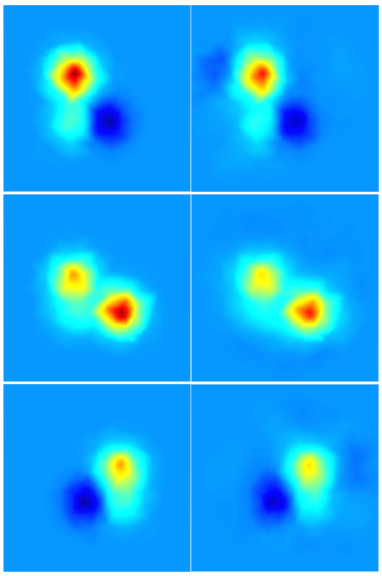

Figure 4: Initial state (left) and the reconstructed state (right) from measurement on the half sphere after 10 iterations.

As far as we know, in practice, it is not possible to measure on a surface. But line detector exists[1], so we can measure the pressure on lines, distributed on a half-sphere. As a first test, we use a very coarse grid of 10 lines detector as shown on Fig. 5, with $\gamma = 1$ (we again use the same noisy observation than for the previous tests, truncated on the grid). In spite of this, we see on Fig. 6 that the reconstructed initial position is sufficient to localize the default of pressure, used to identify sick cells in thermoacoustic tomography.

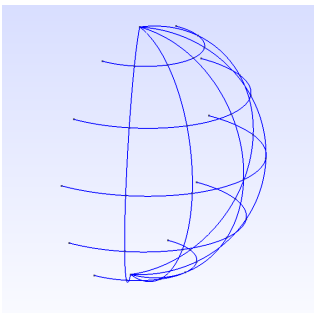

Figure 5: View of the grid used to perform the observation.

[1] See for instance http://www.recendt.at/528_ENG_HTML.php for the recent developments to construct such devices.

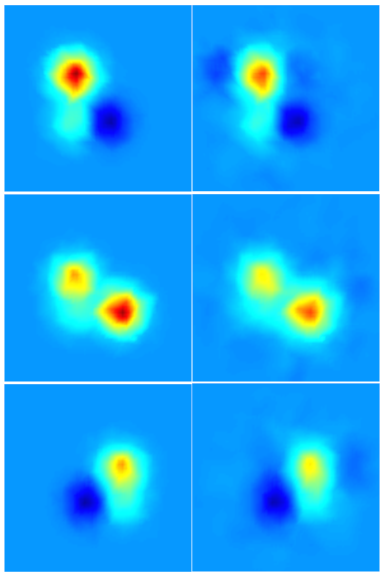

Figure 6: Initial state (left) and the reconstructed state (right) from measurement on a coarse grid along the half sphere after 10 iterations.

Remark that if we do more iterations, we could expect a better reconstruction. However, the relative error will start to increase after some numbers of back and forth cycle of observers. This phenomena is not due to the specific case we simulated here. In fact, it has been shown by Haine and Ramdani [15] that, numerically, there exists an optimal number of iterations, depending on the mesh parameters in time and space. Using a numerical viscosity method, as in the paper of Ervedoza and Zuazua [7], we can remove this limitation of the approach by the algorithm of [29]. It has been done successfully in a recent work of Garcìa and Takahashi [11].

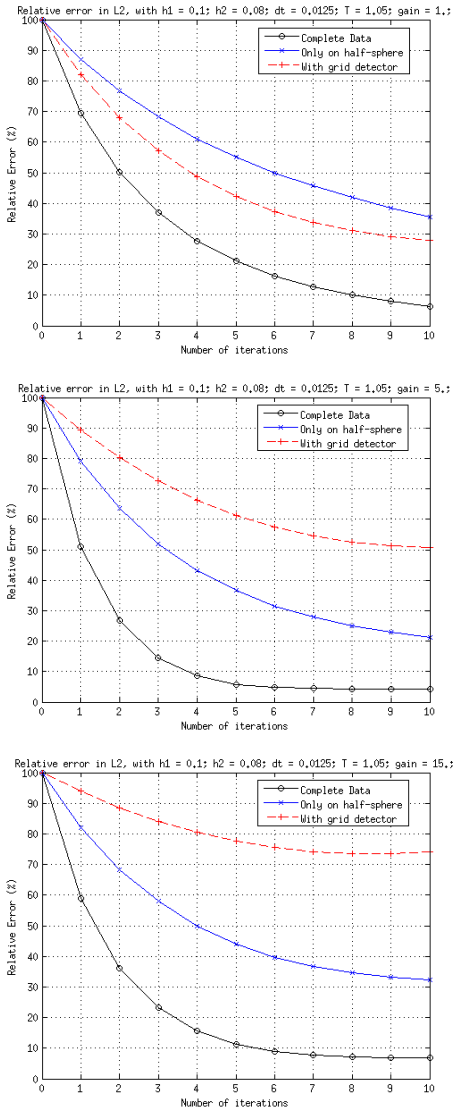

Figure 7: Comparison of the evolution of the relative errors in the three cases, in function of the iterations, with different gain parameter γ (1, 5 and 15).

5. Conclusion

We proposed an alternative and original way to solve thermoacoustic tomography, close to the algorithm of [30] based on Neumann series. However, our method only needs direct wave solver in practice.

Numerical aspects of this approach have to be investigate in future works, especially to improve the computation time, quite expensive for the moment, especially in comparison with the results obtained by Kunyansky in [21]. Furthermore, while the algorithm seems to be robust to Gaussian noise in the numerical tests, theoretical works are needed to add it in the model.

In this work, we add artificial Dirichlet boundary conditions *sufficiently far away* from the support of the initial state. One could ask if these conditions have an influence on the algorithm, especially on the numerical aspects, and if other kind of boundary conditions could lead to a better rate of convergence.

6. Acknowledgment

I wish to thank Philippe Moireau and Dominique Chapelle from Inria M∃DISIM for their fruitful comments, which enabled to speed up the original code, and definitely enhance the simulations in the reconstruction procedure.

References

[1] M. A. Anastasio, J. Zhang, D. Modgil, and P. J. La Rivière, *Application of inverse source concepts to photoacoustic tomography*, Inverse Problems, 23 (2007), pp. S21–S35.

[2] D. Auroux and J. Blum, *Back and forth nudging algorithm for data assimilation problems*, C. R. Math. Acad. Sci. Paris, 340 (2005), pp. 873–878.

[3] D. Auroux, J. Blum, and S. Marinesque, *Data assimilation: variational methods and back and forth nudging algorithm; application to thermoacoustic tomography*, in Proc. 11th International Conference on Mathematical and Numerical Aspects of Waves, 2013, pp. 69–70.

[4] C. Bardos, G. Lebeau, and J. Rauch, *Sharp sufficient conditions for the observation, control, and stabilization of waves from the boundary*, SIAM J. Control Optim., 30 (1992), pp. 1024–1065.

[5] D. Chapelle, N. Cîndea, M. De Buhan, and P. Moireau, *Exponential convergence of an observer based on partial field measurements for the wave equation*, Math. Probl. Eng., (2012), pp. Art. ID 581053, 12.

[6] P. Dular and C. Geuzaine, *GetDP Reference Manual: the Documentation for GetDP, a General Environment for the Treatment of Discrete Problems*. http://www.geuz.org/getdp/.

[7] S. Ervedoza and E. Zuazua, *Uniformly exponentially stable approximations for a class of damped systems*, J. Math. Pures Appl. (9), 91 (2009), pp. 20–48.

[8] L. C. Evans, *Partial differential equations*, vol. 19 of Graduate Studies in Mathematics, American Mathematical Society, Providence, RI, 1998.

[9] M. Fink, *Time reversal of ultrasonic fields–basic principles*, IEEE Trans. Ultrasonics Ferro-electric and Frequency Control, 39 (1992), pp. 555–556.

[10] M. Fink, D. Cassereau, A. Derode, C. Prada, O. Roux, M. Tanter, J.-L. Thomas, and F. Wu, *Time-reversed acoustics*, Rep. Prog. Phys., 63 (2000), pp. 1933–1995.

[11] G. C. García and T. Takahashi, *Numerical observers with vanishing viscosity for the 1d wave equation*, Advances in Computational Mathematics, (2013), pp. 1–35.

[12] B. Gebauer and O. Scherzer, *Impedance-acoustic tomography*, SIAM J. Appl. Math., 69 (2008), pp. 565–576.

[13] C. Geuzaine and J.-F. Remacle, *Gmsh: A 3-D finite element mesh generator with built-in pre- and post-processing facilities*, International Journal for Numerical Methods in Engineering, 79 (2009), pp. 1309–1331.

[14] G. Haine, *Recovering the observable part of the initial data of an infinite-dimensional linear system with skew-adjoint generator*, Mathematics of Control, Signals, and Systems, (2014), pp. 1–28.

[15] G. Haine and K. Ramdani, *Reconstructing initial data using observers: error analysis of the semi-discrete and fully discrete approximations*, Numerische Mathematik, 120 (2012), pp. 307–343.

[16] P. Hébrard and A. Henrot, *Optimal shape and position of the actuators for the stabilization of a string*, Systems Control Lett., 48 (2003), pp. 199–209. Optimization and control of distributed systems.

[17] Y. Hristova, *Time reversal in thermoacoustic tomography - an error estimate*, Inverse Problems, 25 (2009), pp. 055008, 14.

[18] K. Ito, K. Ramdani, and M. Tucsnak, *A time reversal based algorithm for solving initial data inverse problems*, Discrete Contin. Dyn. Syst. Ser. S, 4 (2011), pp. 641–652.

[19] P. Kuchment and L. Kunyansky, *Mathematics of thermoacoustic tomography*, European J. Appl. Math., 19 (2008), pp. 191–224.

[20] L. Kunyansky, *A series solution and a fast algorithm for the inversion of the spherical mean radon transform*, Inverse Problems, 23 (2007), pp. S11–S20.

[21] ———, *Fast reconstruction algorithms for the thermoacoustic tomography in certain domains with cylindrical or spherical symmetries*, Inverse Probl. Imaging, 6 (2012), pp. 111–131.

[22] ———, *A mathematical model and inversion procedure for magneto-acousto-electric tomography*, Inverse Problems, 28 (2012), pp. 035002, 21.

[23] K. Liu, *Locally distributed control and damping for the conservative systems*, SIAM J. Control Optim., 35 (1997), pp. 1574–1590.

[24] D. Luenberger, *Observing the state of a linear system*, IEEE Transaction on Military Electronics, 8 (1964), pp. 74–80.

[25] A. Münch, P. Pedregal, and F. Periago, *Optimal design of the damping set for the stabilization of the wave equation*, J. Differential Equations, 231 (2006), pp. 331–358.

[26] L. Oksanen and G. Uhlmann, *Photoacoustic and thermoacoustic tomography with an uncertain wave speed*, preprint, (2013).

[27] K. D. Phung and X. Zhang, *Time reversal focusing of the initial state for kirchhoff plate*, SIAM J. Appl. Math., 68 (2008), pp. 1535–1556.

[28] J. Qian, P. Stefanov, G. Uhlmann, and H. Zhao, *An efficient Neumann series-based algorithm for thermoacoustic and photoacoustic tomography with variable sound speed*, SIAM J. Imaging Sci., 4 (2011), pp. 850–883.

[29] K. Ramdani, M. Tucsnak, and G. Weiss, *Recovering the initial state of an infinite-dimensional system using observers*, Automatica, 46 (2010), pp. 1616–1625.

[30] P. Stefanov and G. Uhlmann, *Thermoacoustic tomography with variable sound speed*, Inverse Problems, 25 (2009), p. 075011.